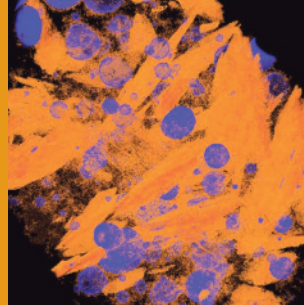


# 3D Analysis of Rock Textures: Quantifying Igneous Microstructures

Dougal A. Jerram<sup>1</sup> and Michael D. Higgins<sup>2</sup>



3D false-colour image of the texture in a lava flow from Teide volcano, Tenerife. Orange: feldspar crystals; blue: vesicle bubbles. The crystals are up to 2 cm long.

**A**n important goal of petrographers is to analyse rock textures (microstructures) and compositions in three dimensions, and thus fully quantify rock properties (porosity and permeability, geochemistry, crystal abundance, etc.). With the advent of serial sectioning techniques, X-ray tomography analysis and advanced image analysis, it is becoming increasingly easy to reconstruct rock textures in three dimensions. An exciting consequence is the potential to reconstruct crystal populations in three dimensions and relate their distribution to the chemical budget of a rock. Here we review the current state of the art in textural analysis techniques and consider the possibilities of virtual three-dimensional models of rock textures.

KEYWORDS: 3D textures, microstructure, X-ray tomography, petrography, serial sectioning

## INTRODUCTION

Although the patterns and structures of rocks have been observed and recorded since the Classical age of Greece, it was in the nineteenth century that the development of the polarising microscope enabled a vast increase in the number and detail of petrological studies (see review by Merriam 2004). At that time petrographic observations, such as estimates of average grain size, grain relationships, grain boundary shapes and orientation fabrics, were mostly qualitative. While qualitative data have their uses, they cannot constrain physical models of processes like quantitative data can, and the seminal work by Chayes (1956) on petrographic modal analysis paved the way for a more robust statistical approach to quantitative petrology. With the increasing power of imaging technologies, plus improved computer processing and modelling, a new petrological approach to two-dimensional (2D) and more recently three-dimensional (3D) textural analysis of rocks is emerging (Fig. 1; Jerram and Kent 2006). This approach is the topic of this contribution.

The texture<sup>3</sup> of rocks and other crystalline materials can be quantified by measuring such parameters as size, shape, orientation and position of common components, e.g. crystals, pores and fractures (e.g. Jerram et al. 1996; Brandon and Kaplan 1999; Higgins 2006). These parameters are derived from 3D structures within the rock, and hence it is desirable that rocks should be examined using 3D analytical methods.

<sup>1</sup> Dept. of Earth Sciences, Durham University  
South Rd, Durham DH1 3LE, UK  
E-mail: D.A.Jerram@dur.ac.uk

<sup>2</sup> Université du Québec à Chicoutimi, 555 blvd de l'Université  
Chicoutimi, Québec G7H 2B1, Canada  
E-mail: mhiggins@uqac.ca

<sup>3</sup> Materials scientists and some geologists prefer the terms *microstructure* or *fabric* to *texture*. Similarly materials scientists use the term *polycrystalline* for a material containing more than one crystal.

Such methods are based on the attenuation of beams that penetrate the sample (e.g. X-ray tomography) or on the reconstruction of the sample from a series of parallel sections (e.g. serial sectioning, confocal scanning laser microscopy).

3D methods are not always applicable: samples and grains may be too large or small; the method may be so expensive that sufficient crystals and samples cannot be analysed; and many 3D methods (e.g. beam techniques) cannot distinguish touching grains of the same mineral, clearly separate different minerals with very similar properties,

or determine the orientation of the crystal lattice. Hence, it may be necessary to study 2D sections through a rock and extrapolate these data to obtain three-dimensional textural parameters using stereological methods (Underwood 1970; Exner 2004). This has been the more common approach in the past and forms the foundation from which many 3D textural studies can be interpreted (Higgins 2006 and references therein). In the following sections we introduce the various techniques available for reconstructing 3D rock textures, with particular attention to serial section and X-ray tomographic methods, and we review how they can be applied to the quantification of 3D rock textures.

## DIRECT 3D ANALYTICAL METHODS

### *Serial Sectioning*

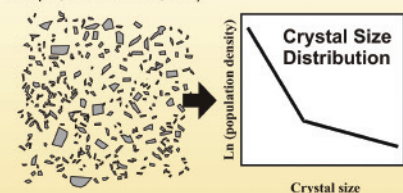
The texture of a rock sample can be established from serial sectioning (Bryon et al. 1995) or serial grinding (e.g. Marschallinger 1998; Mock and Jerram 2005), followed by computer reconstruction. Initially, a surface is cut and imaged with a camera or scanner. The surface may also be stained to emphasise a particular mineral – for instance the well-known sodium cobaltinitrite treatment for K-feldspar. In serial grinding, the surface is then ground away and a new surface made, parallel to the original section, and the process is repeated to provide a number of serial section images through the sample (Fig. 2); the material between sections is destroyed with only the image of the section remaining. By using an annular or diamond wire saw, it is also possible to prepare a series of parallel thin sections through the rock. This has the advantage that the sample is not completely destroyed, enabling geochemical analysis of the resultant sections in the context of the 3D texture.

In principle the datasets can be made with very high resolution and precision. The resolution of the method is limited by the spacing of the sections (which can be set using jigs

## 2D textural analysis and stereological methods

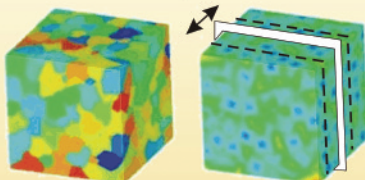
Measurement of 2D intersection parameters in thin sections (long axis, shape, orientation, etc)

Conversion to 3D using stereology



## 3D textural analysis by direct methods

Measurement of 3D parameters using X-ray tomography or serial section reconstructions. Individual crystals can be identified directly and measured for shape, size, etc.



### Special Features

- Cheap optical microscopes are readily available
- Optical methods are well known
- Global parameters (e.g. phase abundance) can be precisely determined
- Lattice orientations are commonly available
- Chemical compositions can also be determined
- Direct methods can be used for any shape of crystal or structure
- Individual crystals or other structures can be directly measured
- Typical resolution is as good as  $2\ \mu\text{m}$  for standard micro CT applications
- Very high resolution is possible for small samples using synchrotron analysis

### Limitations

- Stereological conversion necessitates known, regular crystal shapes
- Stereological conversion is less precise for small crystals in population
- Populations of crystals are described statistically, not individually
- Specialised equipment is expensive; limited sample size
- Cannot easily separate touching crystals unless shape is assumed
- Lattice orientations are inaccessible
- Not always possible to identify different minerals

**FIGURE 1** Comparison of the common approaches in 2D and 3D textural analysis

for serial lapping giving a possible spacing of a few microns; FIG. 2). If one wishes to reconstruct a rock volume in which the voxels (3D pixels) have the same resolution in all directions, the sections would be ground at the spacing of the resolution of each image (Marschallinger 1998). This technique allows the study of a full 3D volume of the rock (discussed below under X-ray tomography). If the objects to be analysed are relatively coarse grained, less resolution in the grinding direction can be used to increase the volume of material sampled and reduce the size of the dataset (e.g. Mock and Jerram 2005). Although the process of serial grinding and lapping is very time consuming, it can give excellent results, especially for small numbers of irregularly shaped objects. Resolutions as small as  $40\ \mu\text{m}$  have been achieved in such studies (e.g. Marschallinger 1998), which is comparable to the resolution of some of the low-resolution X-ray tomographic datasets (see later sections). In the case of serial thin sections, a much larger spacing of the slices is needed – typically  $>0.5\ \text{mm}$ . However, it is much easier to distinguish separate crystals in thin section than on a rock surface.

Another significant advance is the recent use of fully automated (robotic) systems to reduce sectioning times and improve resolution. The automated serial sectioning device Robo-Met.3D (U.S. Patent Pending) has been developed (Spowart 2006) with the capability of removing sections of

metallic alloys and composites with repeatable section depths from less than  $0.2\ \mu\text{m}$  up to  $10\ \mu\text{m}$ . Although this device has yet to be used for petrography, the flexibility of the adopted serial lapping/polishing approach, coupled with digital optical colour microscopy, has the potential to achieve very high resolution section images over many cubic millimetres of material, at rates up to 20 sections per hour.

The series of sectional images must be processed to separate out the different minerals or structures of interest (FIG. 2). A large number of methods can be used to achieve this, but the most common approach is to classify each pixel on the basis of its colour (Higgins 2006). However, there have been considerable advances in image-recognition algorithms, and we can expect more advances (Sharon et al. 2006). Of course, if thin sections are used then a much larger range of traditional optical methods is possible. The classified sectional images can then be constructed into 3D, either as a data volume (voxel image) or as reconstructed surfaces around sequential sections through individual crystals (e.g. FIG. 2). In either case the resultant 3D image can be used to establish the complete shape of each crystal.

### Tomography

Remote 3D imaging using X-ray tomography was pioneered in the Earth sciences in the 1990s in Bill Carlson's lab in Texas. It is now a growing area of research, with the development of instruments capable of very high resolution analysis. Tomography (CT – computed axial tomography) is the reconstruction of a section (slice) from many separate projections around an object (FIG. 3). A series of closely spaced slices are then assembled into a 3D image. The method is commonly applied using a relatively standard X-ray source (e.g. Ketcham and Carlson 2001), but it can also be used with other sources, such as synchrotron radiation (e.g. Ikeda et al. 2004), gamma rays, electrons and even light. FIGURE 3 shows the stages from image capture through to processing and finally to a reconstructed 3D virtual texture ready for quantification; these stages are explained in detail below.

Minerals and pores are distinguished in X-ray tomography on the basis of their linear attenuation coefficient,  $\mu$ . This parameter depends on the electron density of the mineral, the effective atomic number of the mineral, and the energy of the incoming X-ray beam. In some situations the sample can be examined using X-rays of two different energies (frequencies) and the images combined to increase phase discrimination. In general, this method cannot separate touching crystals of the same mineral because  $\mu$  does not depend on direction, even in anisotropic minerals. This contrasts with the optical anisotropy of most common minerals and the electronic anisotropy of all crystalline materials.

Sample size is limited by the attenuation of X-rays and the physical dimensions of the sample chamber. Some industrial instruments can handle samples up to 40 cm long whereas medical scanners can accommodate much larger samples. Spatial resolution is a function of sample size and the number of pixels in the image (typically 500 to 2000 pixels on a side). The modern micro X-ray tomography

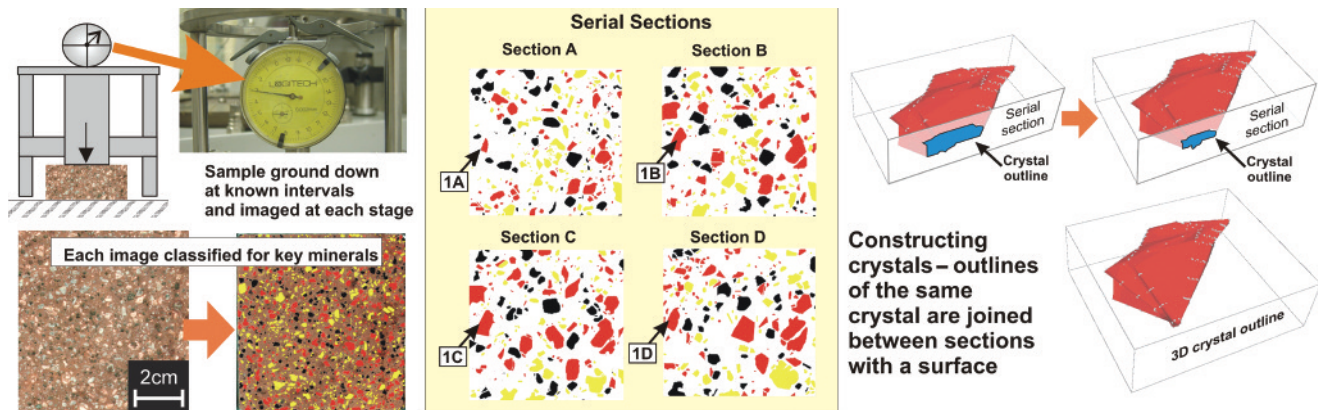


**FIGURE 2** Reconstruction of a 3D texture using serial sectioning-grinding. Sequential sections are made at known spacings through the sample using a jig that can be set to grind down to known intervals. Images are taken from each section as high-resolution scans, and each of the key minerals is identified with a different colour.

Simplified digital serial sections are then used to identify cuts through the same crystal in different sections. In the example shown (adapted from Mock and Jerram 2005), each crystal is reconstructed with an iso-surface, which provides an outline of the crystal volume and shape.

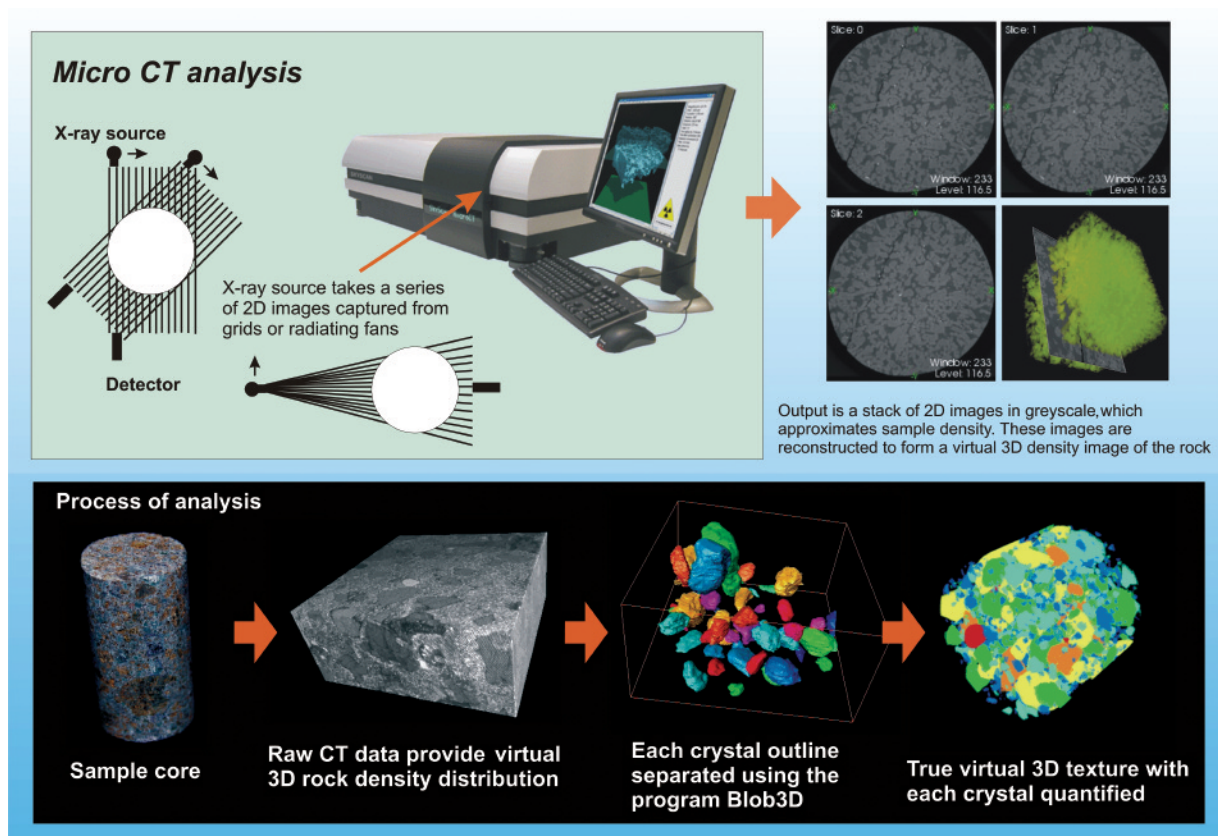


**FIGURE 3** Measuring 3D textures using X-ray CT techniques. X-rays are passed through the sample to produce a series of 2D images that are spaced close to each other (typically at resolutions of 7–30  $\mu\text{m}$ ). Sequential images are captured by rotating the sample or source. The resultant images are a series of spatially constrained, stacked, greyscale tiff files, in which the grey values are related to the linear attenuation coefficient (density) of the material (mineral) at that position in the sample. Images are rendered to pick out key phases for analysis. Using software such as Blob3D (see text), the individual elements of the texture, such as crystals, can be sampled and quantified.

ited by the number of pixels. For example, Godel et al. (2006) used a medical scanner to image sulphides in layered intrusions and achieved voxel sizes of 0.125 mm  $\times$  0.125 mm  $\times$  0.5 mm, for a 10 cm long core.

Synchrotron radiation has some advantages over normal X-rays. For example, synchrotron radiation is very intense and can be focussed in a small volume. Gualda and Rivers (2006) achieved resolutions of 8–17  $\mu\text{m}$  using the synchrotron source at Argonne National Laboratory, for sample cylinders 5–10 mm in diameter. Synchrotron radiation has also been combined with X-ray fluorescence computed tomography to give a 3D compositional map (e.g. Lemelle et al. 2004). Although precision is currently low, this method shows promise for some materials. The highest-resolution electron tomography uses a transmitted electron microscope and can image at the sub-micron to nanometre scale (e.g. Friedrich et al. 2005).

instruments have quoted resolutions in the range of 6–30  $\mu\text{m}$  with core or block sample sizes of 7 cm by 3 cm diameter, and most recent lab systems routinely achieve resolution as low as 5  $\mu\text{m}$ . New nanotomography systems are also arriving on the scene, and these may achieve resolutions as low as 300 nm voxel size. With much larger scans, resolutions are commonly 0.1–0.2 mm for decimetre size samples. Larger samples have a lower resolution, lim-

### Less Commonly Used 3D Methods

Optical scanning can be used to determine the texture of small proportions of crystals in transparent materials. The section is examined with an optical microscope at high magnification with a large aperture. In this situation the depth of field is small and a narrow range of depths in the section are focussed. A photograph is taken and the sample to objective distance increased. The process is repeated to build up a complete 3D reconstruction of the section. The matrix of the crystals must be sufficiently transparent, and the crystal number density must be sufficiently low that the whole crystal can be observed; hence the method can be applied only in special circumstances, for instance in the study of microlites in a glassy volcanic rock (Castro et al. 2003). It is not always necessary to reconstruct the whole 3D structure: the length and other shape parameters can be determined from the vertical and horizontal position of the ends of the crystal.

A scanning laser confocal microscope is designed specifically for this application (e.g. Petford et al. 2001; Bozhilov et al. 2003). Instead of shining a light on the whole section, only a part of the sample is scanned with a laser beam. The image is then reconstructed sequentially, allowing a vertical stack of images (z-series) to be rapidly compiled. This technique is non-destructive, and scattering of light from adjacent crystals and matrix into the volume of interest is much reduced. A confocal study of the porosity distribution in a sandstone from the North Sea is presented in FIGURE 4 (Petford et al. 2001).

Magnetic resonance imaging is used extensively in medical applications but has only recently been applied to textural studies of rocks. Magnetic resonance generates images that largely reflect the hydrogen content of materials. So far this method has only been used to visualize distributions of water-filled pores in carbonate rocks (Gingras et al. 2002), but it may be useful in other studies, especially if the resolution of the method can be improved.

### EXTRACTION OF TEXTURAL PARAMETERS FROM DATA VOLUMES

The analytical methods described above produce as final output a 3D image commonly referred to as a data volume, or data brick. It is comprised of voxels, the volumetric equivalent of pixels in images. Extraction of textural information from data volumes comprises three steps: classification of voxels into minerals, separation of touching crystals, and measurement of crystals (Ketcham 2005). Initially researchers used industrial or medical software designed for imaging and qualitative studies of a limited number of complex structures. However, as petrologists we commonly want to

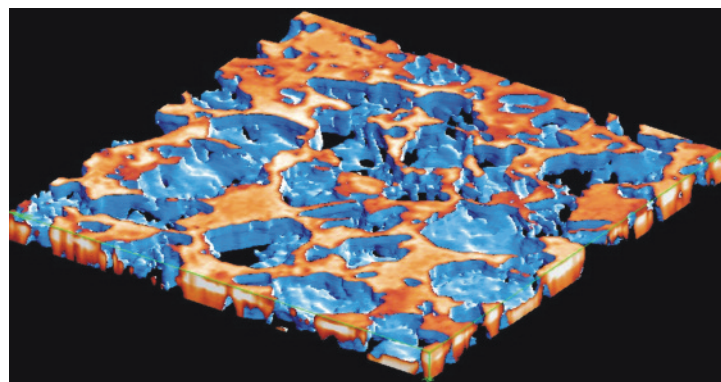


**FIGURE 4** 3D image of porosity (orange) and grains (blue) from a North Sea sandstone, generated using a scanning laser confocal microscope (Petford et al. 2001)

measure the parameters of many individual rock structures (crystals, fractures, etc.) and study the distribution of the textural parameters (size, orientation, etc.). Recently, dedicated geological software has been developed for this purpose (e.g. Ketcham 2005).

### Turning Voxels into Phases

The classification process is commonly the most complex. Data volumes from X-ray tomography are greyscale images (see FIG. 3), with only one value for each voxel. Such images can be segmented by considering a window of acceptable values. Voxels in the interior of ideal crystals will have a narrow range of values of  $\mu$  (e.g. TABLE 1). Voxels on the edge will have  $\mu$  values intermediate between those of the mineral and the host. However, most crystals are not ideal: they may have exsolution lamellae, fractures, alteration, inclusions and zoning. These effects are compounded by analytical 'noise' and lead to a much wider range in  $\mu$  for a mineral (FIG. 5). Ketcham (2005) proposed a number of approaches where the neighbouring voxels are also used to help the classification. For instance, the 'seeded threshold' filter initially accepts voxels within a range of greyscale values. Each object is then expanded by the addition of connected voxels that have a wider range of greyscale values. If the mineral grain is assumed to be spherical, then irregular groups of voxels may be simplified by substituting spheres with volumes equal to that of the original crystal (Carlson et al. 1995).

Once the different phases have been identified, it is possible to colour code them differently to aid with their visualisation/quantification, in effect to give false colour to the greyscales. FIGURE 5 shows different phases (glass, vesicles and minerals) identified from a pumice clast sample in the Bishop Tuff deposit, USA, and graphs of their range in attenuation (Gualda and Rivers 2006). Data volumes derived from serial sectioning potentially have the advantage that the true colour information is also available for each image. This is most helpful to distinguish minerals that would have very similar attenuations in normal X-ray tomography datasets, such as sanidine and plagioclase. When texture colour information from each slice is included in the 3D volume, there are at least three colour values for each voxel, and more complex numerical methods can be applied for classifying minerals (Higgins 2006).

### Separation

Touching crystals or grains are not separated by most 3D analytical methods; hence separation must be done during data reduction. Voxel groups can be examined individually and cut apart manually (Ketcham 2005). In an automatic process suggested by Prousevitich and Sahagian (2001), interconnected voxel clusters are 'peeled' or eroded until the individual objects are separated, and finally the crystal centres are defined. The crystals are then rebuilt using an assumed shape, such as a sphere or an equidimensional polyhedron. Another approach is to use the 'watershed' algorithm. The acceptable range of voxels in a group is reduced until the group separates into distinct objects. The voxel group is then rebuilt from these centres (Ketcham 2005). Once individual grains within a sample have been identified, they can also be false coloured to highlight each different mineral (e.g. FIG. 3) for analysis.

### Measurement

Measurement of the dimensions of separated groups of voxels is conceptually simple but has not been facilitated by current software, which is designed for industrial and medical applications. An exception is the program Blob3D (Ketcham 2005).

**TABLE 1** SPECIFIC GRAVITY, MEAN ATOMIC NUMBER (MAN) AND LINEAR ATTENUATION COEFFICIENT ( $\mu$ ) FOR PHASES IN THE BISHOP TUFF. From Gualda and Rivers (2006)

Mineral	Specific gravity	Percent density difference (rel. quartz)	Mean atomic number ( $\bar{Z}$ )	Percent MAN difference (rel. quartz)	$\mu$ ( $\text{cm}^{-1}$ )	Percent $\mu$ difference (rel. quartz)
Quartz	2.65	0	10.8	0	5.4	0
Plagioclase ( $\text{An}_{20}$ )	2.65	0	11.0	1	5.7	6
Sanidine ( $\text{Or}_{65}$ )	2.6	-2	11.5	6	6.7	23
Biotite (Annite)	3.3	25	16.0	48	28	415
Magnetite	5.2	96	21.0	95	79	1358

3D volume clipped for vesicles & glass    3D volume clipped for mineral phases

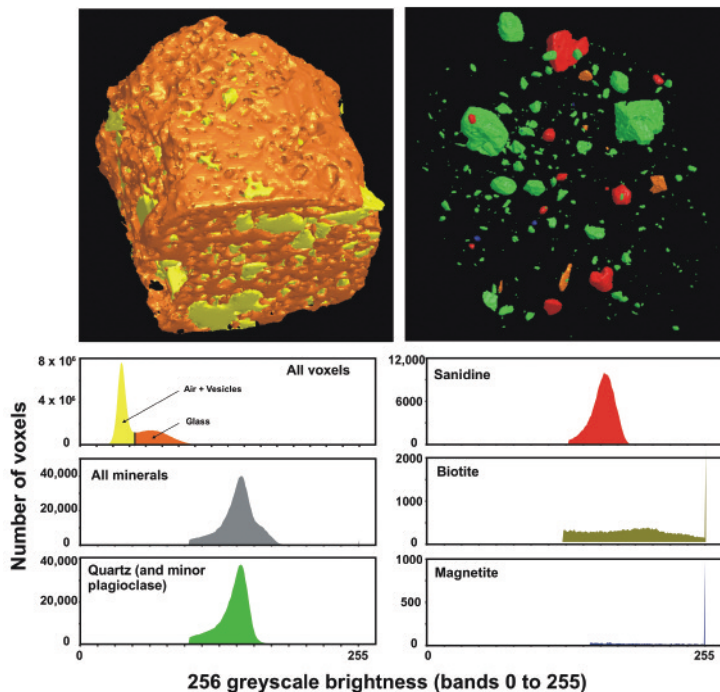


**FIGURE 5** Linear attenuation coefficients of phases in a rhyolite pumice, scaled to 256 brightness levels (data from Gualda; adapted from Gualda and Rivers 2006). 3D volume images show the dataset with voxels representing vesicles and glass removed to highlight the mineral phases (colour codes match between graphs and 3D images). Quartz and sanidine have overlapping brightness ranges. Biotite and magnetite have huge ranges in brightness.

3D measurements produce data on individual crystals, in contrast to the grouped or population data from stereologically corrected sectional data (e.g. Higgins 2000). Hence, for crystal size distributions (CSD) the population density can be determined by differentiation of the cumulative distribution of crystals, as was originally proposed by Marsh (1988). This will produce a smooth CSD, rather than the binned data with which we are more familiar. Of course points will be widely spaced for large (and possibly small) crystals, and there is no accepted criterion for assigning a data cut-off. This may be why some authors continue to use binned data (Gualda 2006). Perhaps a graph that combines the qualities of both approaches will be developed in the future.

### 3D DATASETS: EXAMPLES AND APPLICATIONS

3D datasets from a variety of rocks now exist. These studies focussed on porosity and permeability in sandstones (Petford et al. 2001) and on microstructures, fabrics and size distributions in igneous and metamorphic rocks (e.g. Ketcham et al. 2005; Mock and Jerram 2005; Higgins 2006).

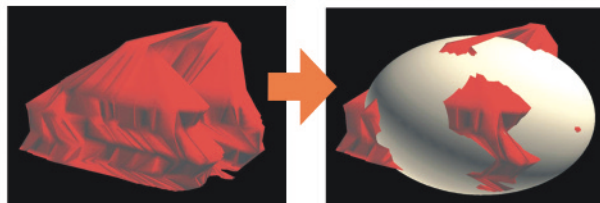
Indeed the methods used in 3D quantification of materials are applicable to a wide range of problems, not just in the Earth sciences, materials science and engineering. Below, we briefly consider some examples of datasets from igneous/volcanic studies.

### Crystal Population Studies and 3D Crystal Shapes

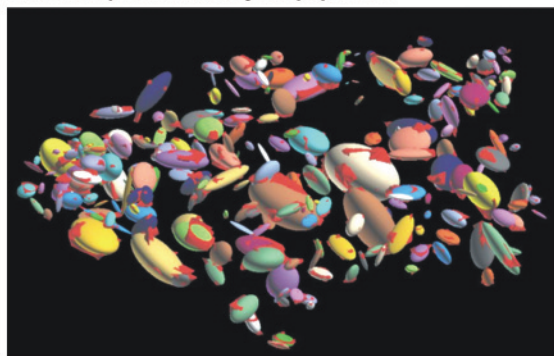
The structural elements of most interest in igneous rocks are crystals, bubbles and inter-crystal pore spaces. They can provide vital information about the textural development and petrogenesis of the rock. Recent 3D studies have examined the measurement of the 3D crystal size distribution in igneous materials using confocal/depth imaging (e.g. Castro et al. 2003), serial grinding (Mock and Jerram 2005) and X-ray tomographic measurements (e.g. Gualda 2006). As discussed above, in such studies the crystal or bubble parameters (shape, size, etc.) are determined from the individual crystal volumes that are measured. Currently, limited data exist for true 3D images of melt-pore space geometries; however, recent 3D textural modelling simulations (e.g. Cheadle et al. 2004; see also Hersum and Marsh 2007 this issue) are providing virtual growth models that will help to constrain how 3D melt-pore space geometries develop, and real 3D measurements of parameters such as dihedral angle (e.g. Holness 2006) provide vital tests for such models.

The 3D volume information obtained for CSD analysis can also be used for the full quantification of true 3D crystal shapes. The shape of crystals is important from a number of perspectives (Kostov and Kostov 1999). The morphology of a crystal growing from a magma depends on the physical conditions that drive its growth (undercooling, melt composition, pressure, etc.). Changes in these conditions will result in changes in the morphology of the resulting crystals. Measuring the 3D shape of a crystal, however, is not a trivial exercise. FIGURE 6 illustrates how the morphology of a crystal can be defined by fitting a best-fit ellipsoid to the crystal volume. This allows us to define the crystal in terms of long, intermediate and short axes. These can be easily visualised on a Zingg diagram (FIG. 6c), which shows how crystal shapes vary within the population and among different populations. Can the 3D crystal shape be used to gain information about the physical conditions of the magma? As yet datasets are limited, but existing information on 3D crystal populations provided by Mock and Jerram (2005) and Gualda and Rivers (2006) (FIG. 6c) suggests that the 3D morphology of crystals within a population varies markedly. If this is the case for all volcanic systems, then such varied shapes may represent a mixture of crystals from different portions of the magma chamber where different physical conditions exist, or they may indicate that overall changes in the physical conditions of the magma body have occurred through the nucleation and growth history of the crystal population. As the number of crystal shape datasets increases from well-constrained volcanic systems, we will be able to assess the importance of crystal shapes more clearly.

**A** Long, intermediate, and short axes of complex crystal volume determined by a best-fit ellipsoid



**B** Best-fit ellipsoids for a crystal population



**C** 3D shape distribution: Zingg diagram

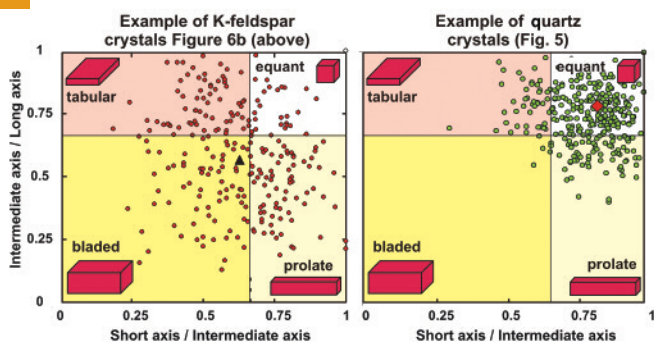


**FIGURE 6** Quantifying the 3D shape of crystals in a rock (modified from Mock and Jerram 2005). (A) Complex crystal shapes can be defined in terms of the long, intermediate and short axes by applying a best-fit ellipsoid to the volume defining the crystal shape. (B) Ideally more than ~250 crystals should be sampled to get a statistical representation of the shape variation within the sample. (C) Finally the shape data, in terms of short, intermediate and long dimensions, can be represented on a Zingg diagram plotting intermediate/long axis versus short/intermediate axis to distinguish if the crystals are equant, tabular, prolate or bladed as defined by shaded areas. In the K-feldspar example, the average shape is indicated by a black triangle and in the quartz example, by a red diamond.

**The Future of 3D Textural Quantification and Visualisation – A Combined Textural and Geochemical Framework?**

Full quantification of the textural parameters of a rock sample at very high resolutions plus improved methods of micro-geochemical analysis of within-crystal variations in major, trace and isotope elemental data (see Davidson et al. 2007 this issue) pave the way for future 3D quantification of rocks. Just how will we be able to use such data in real cases? FIGURE 7 shows how the joint application of 3D textural quantification and micro-analytical geochemistry can be used to examine the role of ‘antecrysts’ (recycled crystals) in volcanic rocks. Using 3D volume data from X-ray tomography, it is possible to identify the large crystal fraction representing the recycled crystals in the sample. The sample can then be correctly oriented to produce the ‘ideal’ section through these crystals for microgeochemical analysis. With the full

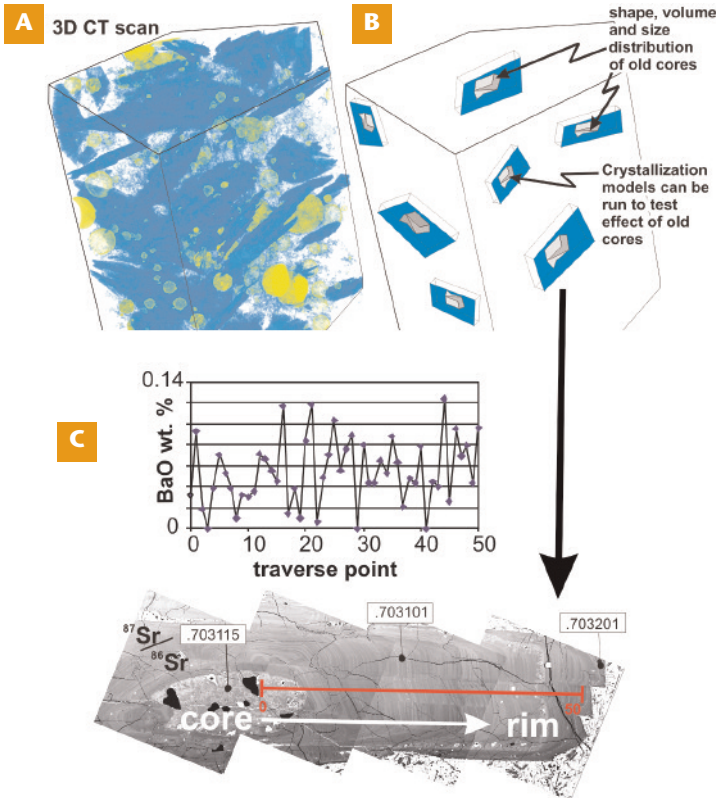


**FIGURE 7** Combining 3D textural information with high-resolution geochemistry. The example shows a 3D X-ray CT scan through a sample from a lava flow from Teide volcano. (A) The scan reveals the distribution of feldspar crystals (blue) and vesicles (yellow/green). (B) Within the crystal population, a number of large crystals contain old cores (recycled in the magma system; crystals up to 2 cm long). These recycled crystals (‘antecrysts’) are targeted because they contain multiple records of the magma system through time. (C) Detailed microgeochemical analysis reveals the history recorded by these large crystals (example shows Ba concentration and Sr isotope ratio variations from core to rim). With a fully quantified 3D texture, the amount and volume of core to rim variations can be calculated.

3D distribution of the recycled crystals known, it is possible to assess their contribution to the overall chemical budget of the rock and to the evolution of the crystal population.

Additionally the routine collection of X-ray tomography data from a sample before sectioning for geochemical analysis can prove to be a very powerful aid in locating and visualizing crystals for analysis, and the sample can then be sectioned in the correct orientation to maximise the geochemical data. 3D visualisation ‘caves’ (FIG. 8) provide a virtual tour through a rock’s texture, allowing examination of different textural elements, e.g. crystals and vesicles in the example from Teide volcano (FIGS. 7 AND 8). Advances in 3D data collection, resolution and scope of data analysis, combined with the cost reduction due to technical advances, make this an exciting area of study in the modern petrological analysis of rocks. As more 3D datasets of key rock textures emerge, we will start to open up some of the secrets contained within these fascinating microstructures, bringing geochemistry and geochronology into the 3D realm and pushing forward a new frontier in the world of modern petrology.



**FIGURE 8** X-ray CT 3D rock texture being explored using a state-of-the-art 3D visualisation system at Durham University. The rock is a lava from Teide volcano. Feldspar crystals are shown in yellow and vesicles in blue.

## ACKNOWLEDGMENTS

We would like to thank Guilherme Gualda and Nick Petford for constructive comments on the initial draft of this contribution. DAJ would specifically like to thank Alex Mock, Dan Morgan and Darren Chertkoff for assistance on various aspects of the data and examples presented here, Graham Davis (MicroCT lab, Queen Mary, University of London) for 3D data acquisition and Nick Holliman (E-Science visualisation centre, Durham) for help with 3D visualisation. DAJ would like to acknowledge the support of NERC, EU 5th Framework and DeBeers in his textural research. ■

## REFERENCES

- Bozhilov KN, Green HW II, Dobrzhinetskaya LF (2003) Quantitative 3D measurement of ilmenite abundance in Alpe Arami olivine by confocal microscopy: Confirmation of high-pressure origin. *American Mineralogist* 88: 596-603
- Brandon D, Kaplan WD (1999) Microstructural Characterization of Materials. John Wiley & Sons Ltd., Chichester, England, 424 pp
- Bryon DN, Atherton MP, Hunter RH (1995) The interpretation of granitic textures from serial thin sectioning, image analysis and three-dimensional reconstruction. *Mineralogical Magazine* 59: 203-211
- Carlson WD, Denison C, Ketcham RA (1995) Controls on the nucleation and growth of porphyroblasts: Kinetics from natural textures and numerical models. *Geological Journal* 30: 207-225
- Castro JM, Cashman KV, Manga M (2003) A technique for measuring 3D crystal-size distributions of prismatic microlites in obsidian. *American Mineralogist* 88: 1230-1240
- Chayes F (1956) *Petrographic Modal Analysis*. Chapman and Hall, London, 113 pp
- Cheadle MJ, Elliott MT, McKenzie D (2004) Percolation threshold and permeability of crystallizing igneous rocks: The importance of textural equilibrium. *Geology* 32: 757-760
- Davidson JP, Morgan DJ, Charlier BLA (2007) Isotopic microsampling of magmatic rocks. *Elements* 3: 253-259
- Exner HE (2004) Stereology and 3D microscopy: Useful alternatives or competitors in the quantitative analysis of microstructures? *Image Analysis and Stereology* 23: 73-82
- Friedrich H, McCartney MR, Buseck PR (2005) Comparison of intensity distributions in tomograms from BF TEM, ADF STEM, HAADF STEM, and calculated tilt series. *Ultramicroscopy* 106: 18-27
- Gingras MK, MacMillan B, Balcom BJ (2002) Visualizing the internal physical characteristics of carbonate sediments with magnetic resonance imaging and petrography. *Bulletin of Canadian Petroleum Geology* 50: 363-369
- Godel B, Barnes S-J, Maier WD (2006) 3-d distribution of sulphide minerals in the Merensky Reef (Bushveld Complex, South Africa) and the J-M Reef (Stillwater Complex, USA) and their relationship to microstructures using X-ray computed tomography. *Journal of Petrology* 47: 1853-1872
- Gualda GAR (2006) Crystal size distributions derived from 3D datasets: Sample size versus uncertainties. *Journal of Petrology* 47: 1245-1254
- Gualda GAR, Rivers M (2006) Quantitative 3D petrography using X-ray tomography: Application to Bishop Tuff pumice clasts. *Journal of Volcanology and Geothermal Research* 154: 48-62
- Hersum TG, Marsh BD (2007) Igneous Textures: On the kinetics behind the words. *Elements* 3: 247-252
- Higgins MD (2000) Measurement of crystal size distributions. *American Mineralogist* 85: 1105-1116
- Higgins MD (2006) *Quantitative Textural Measurements in Igneous and Metamorphic Petrology*. Cambridge University Press, Cambridge, UK, 276 pp
- Holness MB (2006) Melt-solid dihedral angles of common minerals in natural rocks. *Journal of Petrology* 47: 791-800
- Ikeda S, Nakano T, Tsuchiyama A, Uesugi K, Suzuki Y, Nakamura K, Nakashima Y, Yoshida H (2004) Nondestructive three-dimensional element-concentration mapping of a Cs-doped partially molten granite by X-ray computed tomography using synchrotron radiation. *American Mineralogist* 89: 1304-1313
- Jerram DA, Kent AJR (2006) An overview of modern trends in petrography: Textural and microanalysis of igneous rocks. *Journal of Volcanology and Geothermal Research* 154: vii-ix
- Jerram DA, Cheadle MJ, Hunter RH, Elliott MT (1996) The spatial distribution of grains and crystals in rocks. *Contributions to Mineralogy and Petrology* 125: 60-74
- Ketcham RA (2005) Computational methods for quantitative analysis of three-dimensional features in geological specimens. *Geosphere* 1: 32-41
- Ketcham RA, Carlson WD (2001) Acquisition, optimization and interpretation of X-ray computed tomographic imagery: applications to the geosciences. *Computers & Geoscience* 27: 381-400
- Ketcham RA, Meth C, Hirsch DM, Carlson WD (2005) Improved methods for quantitative analysis of three-dimensional porphyroblastic textures. *Geosphere* 1: 42-59
- Kostov I, Kostov RI (1999) *Crystal Habits of Minerals*. Bulgarian Academic Monograph 1, Prof. Marin Drinov Academic Publishing House; Pensoft Publishers, Sofia, 415 pp
- Lemelle L, Simionovici A, Truche R, Rau C, Chukalina M, Gillet P (2004) A new nondestructive X-ray method for the determination of the 3D mineralogy at the micrometer scale. *American Mineralogist* 89: 547-553
- Marschallinger R (1998) Correction of geometric errors associated with the 3-D reconstruction of geological materials by precision serial lapping. *Mineralogical Magazine* 62: 783-792
- Marsh BD (1988) Crystal size distribution (CSD) in rocks and the kinetics and dynamics of crystallization I. Theory. *Contributions to Mineralogy and Petrology* 99: 277-291
- Merriam DF (2004) The quantification of geology: from abacus to Pentium: A chronicle of people, places, and phenomena. *Earth-Science Reviews* 67: 55-89
- Mock A, Jerram DA (2005) Crystal size distributions (CSD) in three dimensions: Insights from the 3D reconstruction of a highly porphyritic rhyolite. *Journal of Petrology* 46: 1525-1541
- Petford N, Davidson G, Miller JA (2001) Investigation of the petrophysical properties of a porous sandstone sample using confocal scanning laser microscopy. *Petroleum Geoscience* 7: 99-105
- Proussevitch AA, Sahagian DL (2001) Recognition and separation of discrete objects within complex 3D voxelized structures. *Computer & Geosciences* 27: 441-454
- Sharon E, Galun M, Sharon D, Basri R, Brandt A (2006) Hierarchy and adaptivity in segmenting visual scenes. *Nature* 442: 810-813
- Spowart JE (2006) Automated serial sectioning techniques for 3-D analysis of microstructures. *Scripta Materialia* 55: 5-10
- Underwood EE (1970) *Quantitative stereology*. Addison-Wesley Publishing Co., Reading, USA, 274 pp ■